



Published in final edited form as:

Curr Biol. 2017 September 11; 27(17): 2623–2629.e2. doi:10.1016/j.cub.2017.07.019.

Differential phase arrangement of cellular clocks along the tonotopic axis of the mouse cochlea *ex vivo*

Jung-sub Park^{1,4,#}, Christopher R. Cederroth^{1,#}, Vasiliki Basinou^{1,#}, Lara Sweetapple¹, Renate Buijink², Gabriella B. Lundkvist^{1,3,5}, Stephan Michel², Barbara Canlon^{1,*}

¹Department of Physiology and Pharmacology, Karolinska Institutet, 17177 Stockholm, Sweden

²Department of Molecular Cell Biology, Leiden University Medical Center, 2333 ZC Leiden, The Netherlands

³Department of Neuroscience, Karolinska Institutet, 17177 Stockholm, Sweden

⁴Department of Otolaryngology, Ajou University School of Medicine, 164, Worldcup-ro,

Yeongtong-gu, Suwon, 16499, Korea ⁵Max Planck Institute for Biology of Ageing, 50931 Cologne, Germany

Summary

Topological distributions of individual cellular clocks have not been demonstrated in peripheral organs. The cochlea displays circadian patterns of core clock gene expression [1, 2]. PER2 protein is expressed in the hair cells and spiral ganglion neurons of the cochlea in the spiral ganglion neurons [1]. To investigate the topological organization of cellular oscillators in the cochlea, we recorded circadian rhythms from mouse cochlear explants using highly sensitive real-time tracking of PER2::LUC bioluminescence. Here, we show cell-autonomous and self-sustained oscillations originating from hair cells and spiral ganglion neurons. Multi-phased cellular clocks were arranged along the length of the cochlea with oscillations initiating at the apex (low frequency region) and travelling towards the base (high frequency region). Phase differences of 3 hours were found between cellular oscillators in the apical and middle regions and from isolated individual cochlear regions, indicating that cellular networks organize the rhythms along the tonotopic axis. This is the first demonstration of a spatiotemporal arrangement of circadian clocks at the cellular level in a peripheral organ. Cochlear rhythms were disrupted in the presence of either voltage-gated potassium channel blocker (TEA) or extracellular calcium chelator (BAPTA) demonstrating that multiple types of ion channels contribute to the maintenance of coherent rhythms. In contrast, preventing action potentials with tetrodotoxin (TTX) or interfering with cell-to-cell communication the broad-spectrum gap junction blocker (CBX, Carbenoxolone), had no influence on cochlear rhythms. These findings highlight a dynamic regulation and longitudinal distribution of cellular clocks in the cochlea.

* Lead Contact: Professor Barbara Canlon, Department of Physiology and Pharmacology, Karolinska Institutet, Stockholm, 17177, Sweden, +46 8 52487248, Barbara.Canlon@ki.se.

#Equal contribution

Author Contributions

B.C., C.R.C., J.S.P., V.B., S.M., and G.S.L. designed the research. J.S.P., C.R.C., B.C., V.B., L.S. and R.B. performed research. B.C., J.S.P., C.R.C., V.B., R.B., L.S. and S.M. analyzed data. B.C., J.S.P., C.R.C. and V.B. wrote the manuscript.

Keywords

Cochlea; tonotopy; Period 2; circadian rhythm; cellular oscillators; bioluminescence imaging

Results

Robust cell-autonomous PER2::LUC rhythms in the cochlea

Using a bioluminescence imaging system, the spatial distribution of cochlear PER2 rhythms was captured (see methods for details). Clear bioluminescence signals appeared in the cochlea *ex vivo* preparation (Figure S1). Signal intensity analysis of thirteen randomly chosen regions of interest (ROI, approximately 20 to 60 cells) revealed overt oscillations with a period of ~ 24 hours (24.63 ± 1.07 , mean \pm SD, $n = 3$ cochleae, Fig. 1A top). Visual examination of the cochlear explant, at the onset of recording, confirmed that the PER2 bioluminescence was originating from hair cells and spiral ganglion neurons, corresponding to the previously reported PER2 protein expression in the cochlea [1]. Corroborating the whole cochlear oscillations [1], the peak PER2 expression appeared in the subjective night (Fig. 1B) and reached the trough in the subjective day (Fig. 1C). Individual ROIs showed variable peak and trough phases, which indicated large heterogeneity across the preparation. During the second circadian cycle (24–48 h), the total luminescence intensity peaked at 32 h after the beginning of recordings with a peak range of 29–38 h (Fig. 1A). By visual analysis of the image series, the luminescence signals first appeared in the apex and then spread towards the middle turn of the cochlea, suggesting a longitudinal gradient of PER2 rhythms (Movie S1).

Longitudinal arrangement of cell oscillators in the cochlea

We next determined the dynamics of PER2 rhythms at the single-cell level and found that 67 % of PER2::LUC expressing cells displayed robust circadian oscillations (293 out of 438 cells from 5 different preparations, Fig. 1D–F). Representative heat maps (Fig. 1D) and oscillation curves (Fig. 1E) obtained from 3 different preparations over a period of 72 h shows that the peak time of the PER2::LUC expression was variable between different cells as demonstrated across various cycles (Fig. 1E). Quantification of peak-time expression during the second cycle revealed that 67 % of the oscillating cells were peaking between 36 and 48 h and 33 % between 48 and 60 h (Fig. 1F). Similar peak-time variations were observed on the first and third circadian cycles (Fig. 1F). Together with the time-lapsed movie showing a longitudinal PER2 wave, the peak time variation suggested that there could be a gradient of PER 2 rhythms along the tonotopic axis of the cochlea.

We then examined the oscillating profiles of cells located either in the apical or the middle regions, corresponding to low and high frequency sounds respectively, that were localized in the same focal plane (Fig. 2A). Bioluminescence could not be captured from the base region on the same preparation. Quantification of phase showed a significant phase delay of 2.8 h in cells of the middle turn compared to the apical turn ($p < 0.001$, Fig. 2B). Phase differences were apparent between apical and middle regions at 48 hours shown in Fig. 2C, D. The apical population had an average phase of 44.78 ± 2.11 hours with 87.5% of the cells peaking between 36 and 48 hours and 14.28% of the cells peaking between 48 and 60 hours

(Fig. 2E, $n = 56$ cells). The middle turn population had an average phase of 47.58 ± 1.95 hours with 38.89% of the cells peaking between 36 and 48 hours and 61.11% of the cells peaking between 48 and 60 hours (Fig. 2E, $n = 36$ cells). Such apical to middle turn differences were also observed from comparisons in different ROIs (apical turn: $28.09 \text{ h} \pm 2.77$ from the start of recording, mean \pm SD, $n = 11$; middle turn: $31.56 \text{ h} \pm 4.93$ from the start of recording, mean \pm SD, $n = 9$ ROI, $p = 0.042$).

The apical turn does not drive the cochlear rhythms

Whether the apical region is required for the generation of the circadian oscillations in the cochlea was tested using a high-throughput photon-counting photomultiplier that captures whole organ bioluminescence. Removing only the apical turn of cochlear explants we found that the lack of apical input did not affect the phase or the period of PER2::LUC rhythms, suggesting that the apical turn does not drive cochlear rhythms (phase: $41.34 \pm 1.49 \text{ h}$ compared to the intact cochlea 41.93 ± 1.35 , mean \pm SD, $n = 4$, $p = 0.31$; period: $24.37 \pm 0.2 \text{ h}$ compared to the intact cochlea 24.27 ± 0.25 , mean \pm SD, $n = 4$, $p = 0.27$ by a t-test). Rather, we hypothesized that the cochlea contains differentially phased cellular networks that integrate into a stable cochlear rhythm. We therefore explored this possibility by measuring the oscillations of the isolated cochlear regions (apical, middle and basal) recorded simultaneously (Fig. 3A). The amplitude of the individual regions was significantly lower than the amplitude of the whole cochlea, due to the lesser amount of tissue, but circadian PER2 rhythms were still clearly detected (Fig. 3B). In the middle turn, a phase delay of 3.26 hours was found compared to the apical turn, corroborating the findings obtained from cellular recordings (Fig. 2). The phase of the middle region was also delayed by 3.49 hours compared to the whole cochlea ($p < 0.001$, $n = 11-13$, Fig. 3C). In addition, the period of the middle turn was longer than the apical turn or the whole cochlea ($p < 0.001$ for both comparisons, $n = 7-10$, Fig. 3D). The basal part also showed some differences in phase and period when compared to the whole cochlea (phase: $p = 0.047$, $n = 11-13$; period: $p = 0.024$, $n = 7-10$, Fig. 3C, D). Thus, multi-phased cellular oscillators are organized in region-specific networks that have different degrees of synchrony along the cochlea. These findings suggest that the coupling between the different regions is required for an integrated and coherent circadian rhythm in the cochlea.

Potassium and calcium channels are required for the maintenance of cochlear rhythms

To determine if intercellular communication was required for the integration of these cellular responses we treated explants with either a voltage-gated sodium channel blocker (tetrodotoxin; TTX; Fig. 4B), an extracellular calcium chelator (1,2-Bis(2-aminophenoxy)ethane- N,N,N',N'-tetraacetic acid; BAPTA; Fig. 4C) or a voltage-dependent potassium channel blocker (tetraethylammonium; TEA; Fig. 4D). The data showed a rapid dampening of oscillations after BAPTA and TEA treatment for 48 h, while TTX did not have any effect compared to controls. Withdrawal of BAPTA or TEA resulted in the restoration of PER2::LUC oscillations, with an amplitude not differing from pretreatment samples (BAPTA, $p = 0.378$; TEA, $p = 0.109$; by t-test; Fig. 4E) suggesting that dampening of cochlear rhythms requires potassium and calcium transmembrane fluxes.

DISCUSSION

Using bioluminescence imaging to determine the endogenous cochlear PER2 rhythms, we were able to detect robust self-sustained cellular oscillators and found a longitudinal distribution of PER2 rhythms along the cochlear tonotopic axis. To our knowledge, this is the first peripheral organ demonstrating a spatiotemporal arrangement of cellular rhythms. Different cell types in the retina have been shown to have different phases but how they are coordinated has not been demonstrated [3]. In the cochlea, tonotopy is a characteristic feature that allows frequency selectivity [4–6]. The mechanical isolation of the apical, middle and basal regions show that whole cochlear synchronicity depends on an integrated interregional communication. A spatiotemporal organization has been reported for the suprachiasmatic nucleus (SCN), where the expression of *Per1* rhythms peaks earlier in the dorsomedial part compared to the ventrolateral part [7, 8]. However, removal of the dorsal part of the SCN did not affect the synchronization of the ventral oscillators [8]. Overall, the integration of signals from the different cochlear regions appears to be required to generate a coherent synchrony of rhythms at the organ level. The physiological significance of having cellular clocks in the cochlea with different peak expression times may be related to a time-dependent regulation of frequency sensitivity, as found for spontaneous otacoustic emissions in humans [9]. It may also be to distribute, in a time-dependent manner, energy expenses throughout the organ in order to avoid metabolic exhaustion. We have previously shown that the presence of a clock in the cochlea is associated with a differential susceptibility to noise between day and night in mice [1]. The presence of an tonotopic arrangement of cellular clocks could imply that the day/night sensitivity to noise trauma is frequency-specific.

Measuring bioluminescence of reporter clock genes or their protein products in *ex vivo* organ cultures has been a well-established approach to investigate the function of peripheral circadian clocks [10, 11]. It is known that organ-specific rhythms emerge from individual cellular oscillators. Whereas the properties of the circadian clock have been well described in isolated fibroblasts [12], *in situ* analysis of cellular oscillators is a more challenging, due the demand for high amplitude bioluminescence signals. Cellular oscillators have been described in bone and tendon explants [13] as well as in the olfactory bulb, lateral habenula, arcuate nucleus, dorsomedial hypothalamus, bed nucleus of the stria terminalis, amygdala, periaqueductal grey, [14–17] and retina [3]. However, to our knowledge, how cellular oscillators in peripheral tissues are organized has not been described. The current understanding of the architecture of cellular networks within tissues derives mainly from studies of the central circadian clock, the SCN, that identified a spatial arrangement of differentially phased individual SCN clocks [8, 18]. It is not fully understood how the SCN maintains synchrony but several mechanisms have been proposed including intercellular coupling, synaptic transmission, paracrine signaling [19, 20] and astrocyte activation [21, 22]. Furthermore, phase shift studies have demonstrated that clock gene expressions in different regions within the rat SCN readjust with different rates [7, 23–25]. Single cells in SCN brain slices from *mPer1::luc* transgenic mice were rhythmic, however, in the presence of TTX, the cellular oscillations were immediately lost demonstrating that cellular communication and electrical activity are essential for circadian rhythmicity [8]. In contrast,

this was not observed in the TTX treated cochlea, suggesting that synchronization of cochlear rhythms does not require Na^{2+} -dependent action potentials.

In the retina, PER2::LUC rhythms do not require communication via melatonin, glutamate, sodium-dependent action potentials or cx36-containing gap junctions [26]. However, dopamine and GABA immediately impaired PER2::LUC rhythms in the retina via D1, GABA_A and GABA_C receptors, respectively [26]. Alternative routes of intercellular communication within the cochlear epithelium include connexin dependent Ca^{2+} wave propagation [27]. Our results buffering extracellular Ca^{2+} with BAPTA indeed indicate that a transmembrane Ca^{2+} flux or mechanotransduction processes are required for cellular rhythms or their temporal coordination [28–30]. The reduction of calcium flux has been shown to act on PER2 rhythms in the SCN [19] and could have similar actions in the cochlea. It is also possible that removing extracellular Ca^{2+} will simply disrupt intercellular junctions in the cochlear tissue [31]. Restoring normal levels of extracellular Ca^{2+} however, led to a swift and full recovery of PER2 rhythmicity, which may be an unlikely result after structural damage. In addition, the cellular circadian clocks also depend on intrinsic properties, like membrane receptors or ion channel activation [32, 33]. Using TEA as a broad-band K^{+} channel antagonist, has been shown to reduce cochlear action potentials, block delayed rectified K^{+} currents, as well as blocking nicotinic cholinergic receptors, confirming that multiple targets could be affected [34–36]. Application of TEA to SCN neurons has been found to abolish day/night differences in membrane properties [37]. Genetic manipulation of neuronal activity in *Drosophila* clock neurons [38] or reducing SCN neuronal activity by lowering extracellular K^{+} [19] results in blunted rhythms of clock genes. Our results show an impairment of cochlear PER2 rhythms under TEA treatment suggesting that membrane excitability is also required for the maintenance of cochlear PER2 oscillations.

Organotypic cultures from a variety of tissues have been performed for the monitoring of PER2::LUC rhythms, however, histology has seldom been reported. The adult cochlea is notoriously difficult to preserve in culture, with hair cells being extremely sensitive to *in vitro* conditions. We found that hair cells persisted until day 3 of culture yet reduced in number (Figure S2). By day 7 of culture, very few hair cells remained while spiral ganglion neurons were maintained. We thus believe that the oscillations recorded at the single cell level (2 days in culture) reflected signals from both hair cells and spiral ganglion neurons, whereas the long-term monitoring for testing the different pharmacological agents is likely emerging spiral ganglion neurons. The fact that PER2::LUC signals can be detected from the cochlea up to 7 days and can be re-set by either a serum change (Fig. 4), dexamethasone [1], or forskolin (unpublished observations), is a strong indication that the circadian signals obtained from the auditory neurons are extremely robust. It is therefore likely that TEA and BAPTA are affecting spiral ganglion neurons. How these communicate between each other and are affected by TEA and BAPTA remains to be clarified.

Given the broad expression pattern of the large number of heterogeneous ion channels within the cochlea [39], further studies are needed to identify the site and type of channel mediating synaptic communication between individual cellular oscillators to compose intercellular synchrony and rhythmicity in the cochlea. The dependency of PER2 rhythms on

K⁺ channel function and transmembrane Ca²⁺ flux indicates that these ions contribute to the self-sustained cochlear rhythms. It is well known that the cochlea relies on gap-junction coupling to maintain auditory function (for example, connexin 26, 29, 30 and 43) [40]. Our pilot experiments using carbenoxolone (CBX), a broad gap-junction inhibitor, showed no effects on the amplitude of the cochlear PER2::LUC oscillations. However, it should be noted that CBX has other targets beyond gap-junctions making interpretations difficult.

In conclusion, bioluminescence imaging and manipulating ion channels allowed us to elucidate a mechanism of cellular communication within the cochlear clock network and these results establish a foundation for understanding how the homeostasis in the peripheral auditory system is maintained. These novel findings reveal that the cochlea possesses a spatial arrangement of cellular clocks that require transmembrane Ca²⁺ flux and K⁺ channel functionality. The identification of the longitudinal organization of circadian rhythms adds another feature to the tonotopic properties of the cochlea including neurotrophins, ion channels and frequency tuning. Future studies aiming to uncover the circadian nature of inter-cellular communication within the cochlea will provide important insight of the signals needed to sustain spatiotemporal order across the organ.

STAR METHODS

CONTACT FOR REAGENT AND RESOURCE SHARING

Further information and requests for resources and reagents should be directed to and will be fulfilled by the Lead Contact, Barbara Canlon (barbara.canlon@ki.se).

EXPERIMENTAL MODEL AND SUBJECT DETAILS

Recordings of circadian oscillations of the PER2 protein were performed using tissues obtained from homozygotic knock-in PERIOD2::LUCIFERASE (PER2::LUC) transgenic mice with a C57BL/6 background [10], generously provided by Prof. J. Takahashi. All experimental procedures on animals were performed in accordance with the guidelines and regulations set forth by Karolinska Institutet and “Stockholm’s Norra Djurförsöksetiska Nämnd”, as well as the Dutch law on Animal welfare and approved by the Dutch government (DEC 11010). Animals had *ad libitum* access water and to food (Lactamin R34, Lantmännen). Temperature was maintained between 19°C and 21°C and lights were on at 6:00 h and off at 18:00 h.

METHOD DETAILS

Bioluminescence imaging for single-cell—Cochlea from male adult mice were dissected from PER2::LUC mice (4–6 weeks old) and cultured organotypically on a Millicell membrane (PICMORG 50; Millipore, Billerica, MA). Organotypic cultures of the cochlea were prepared as described previously [1]. The cochleae were isolated and organotypic cultures were maintained on a Millicell membrane insert. Membrane inserts were placed in a sealed 35 mm dish containing 1.2 mL of Dulbecco’s Modified Eagles Medium (D7777, Sigma-Aldrich) supplemented with 10 mM HEPES-buffer (Sigma-Aldrich), 2% B-27 (Thermo Fisher Scientific, Waltham, MA), 5 U/ml penicillin and 5 µg/ml streptomycin (0.1% penicillin-streptomycin, Sigma-Aldrich) and 0.2 mM D-luciferin

potassium salt (Promega, Madison, WI), adjusted to pH 7.2 with NaOH. Organotypic cochlea cultures were immediately transferred to an upright microscope (BX51WIF, Olympus, Tokyo, Japan) housed in a light tight and temperature controlled chamber 37 °C (Life Imaging Services, Reinach, Switzerland). The microscope was equipped with a long-working distance objective (10x LWD, Olympus), a cooled CCD camera (ORCA UU-BT-1024, Hamamatsu, Japan) and a motorized stage (Luigs & Neumann XY-shifting table 240) as well as focus control (Marzhauser MA-42Z) both connected to an OASIS-4i Four Axis Controller. Bioluminescence images were obtained from cochlear cultures using 60 min exposure times. Focus was adjusted to image PER2::LUC expressing cochlea cells in one focal plane. Cell-like regions were later defined in the off-line analysis and followed in time. Stage and focus position as well as image acquisition were controlled by software (Image Pro Plus, Media Cybernetics, Warrendale, PA; StagePro plug-in, Objective Imaging, Cambridge, UK). From the images, cell-like regions were selected using an in-house written program for analyzing life cell recording (stacks). For convenience we will refer to these cell-like ROIs as “single cells”. The luciferase signal in the hair cells were distinguished from the spiral ganglion neurons by their location. The spiral ganglion neurons are more medial. For every single cell, the average brightness was calculated in each image and the resulting time series were further analyzed using Matlab-based (Mathworks, Natick, MA) scripts. In order to limit noise and augment the efficiency for subsequent analyses, a previously described algorithm [41] was used to smooth and resample the data to one data point per minute. This provides a sinusoid wave for each single cell. Finally, the smoothed data were detrended and normalized using a fourth order polynomial from the TSA toolbox for MATLAB. The processed intensity traces from the single cell rhythms were evaluated on sustained PER2::LUC signal and circadian rhythmicity. Single-cells were only used if the time series contains at least three viable peaks, where peaks are above the trendline and troughs are below this trendline, and the distance between the peaks is on average within the circadian range of 20–28 hours.

Organotypic cochlear explants and analysis—Cochleae were dissected from male PER2::LUC mice (4–6 weeks old) and cultured organotypically on a Millicell membrane (PICMORG 50; Millipore, Billerica, MA). Cochleae were removed from the temporal bone and placed in Hank’s balanced salt solution (HBSS) buffer with supplements pH 7.2 and 285–315 mOsm/Kg. The cochleae were dissected free of the otic capsule bone and stria vascularis and then transferred to the Millicell membrane and kept in culture for minimum 6 days, as described [1]. The cochlea that was placed on the membrane contained the organ of Corti including the modiolus and were kept in culture for minimum 6 days, as described [1]. For bioluminescence imaging of the different cochlear regions, the cochlea were separated into segments (apex, middle and base), by a perpendicular cut. Cochlear explants were treated with 4 mM BAPTA (Tocris Bioscience, Bristol, UK), 25 mM TEA, 0.5 μ M TTX (Sigma-Aldrich, St. Louis, MO) that were dissolved in DMEM-based culture medium, as described [42]. Real-time luciferase reporter technology was used as described previously [42, 43]. Bioluminescence recordings were done in the LumiCycle Luminometer (Actimetrics, Wilmette, IL, USA) that was placed in a 37°C incubator. Analysis of PER2::LUC rhythms (period, amplitude, and phase) was performed by fitting a sine wave to a 24h-running average after subtraction of the baseline, using the Lumicycle Analysis

software (Actimetrics, Wilmette, IL, USA). The first day of measurements was excluded from the analysis. The amplitudes of whole cochlea and three different cochlear regions were calculated from 3 half-cycles (1.5 cycles), as the difference between highest (peak) and lowest (trough) photon count. For the assessment of ion channels, amplitudes were compared with the values from 3 half-cycles immediately before treatment and after washout. The very first peak after washout was excluded. Phase responses were determined as maximum (peak) luminescence between 24 and 48 h after the start of the recording. Five consecutive peaks were used for period calculations.

QUANTIFICATION AND STATISTICAL ANALYSIS

Data are presented as mean \pm SEM. Statistical analyses were performed with GraphPad Prism 6 (GraphPad software). To compare phases in the apical and middle turn cell populations and to assess amplitudes before BAPTA or TEA treatment and after washout, unpaired student *t*-test was used (Figures 2B, *n* = 36–56 cells; Figures 4E, *n* = 4–11 cochleae). A one-way ANOVA was used to compare amplitude, phase and period of PER2::LUC rhythms in the three different cochlear regions (Figure 3B–3D, *n* = 7–13 cochleae).

Supplementary Material

Refer to Web version on PubMed Central for supplementary material.

Acknowledgements

We thank Karima Chergui, Christian Broberger and Håkan Westerblad for sharing reagents and Tony Jimenez-Beristain for technical support and maintenance of the PER2::LUC colony. This work was supported by the Swedish Medical Research Council K2014-99X-22478-01-3 (B.C.), National Institute on Deafness and other Communication Disorders of the National Institutes of Health R21DC013172 (B.C.), National Research Foundation of Korea grant (2014R1A6A3A03058661) funded by the Ministry of Education of the Korean Government (J.S.P.), Karolinska Institutet (B.C., C.R.C.), Tysta Skolan (B.C., J.S.P., C.R.C, G.L), Lars Hiertas Minne (C.R.C.), Magnus Bergvalls (C.R.C.) and Karolinska Institutet, HÖST (Hearing, Otolaryngology, Language and Speech, to V.B).

References

1. Meltser I, Cederroth CR, Basinou V, Savelyev S, Lundkvist GS, and Canlon B (2014). TrkB-mediated protection against circadian sensitivity to noise trauma in the murine cochlea. *Current biology* : CB 24, 658–663. [PubMed: 24583017]
2. Basinou V, Park JS, Cederroth CR, and Canlon B (2016). Circadian regulation of auditory function. *Hearing research*.
3. Besharse JC, and McMahon DG (2016). The Retina and Other Light-sensitive Ocular Clocks. *J Biol Rhythms* 31, 223–243. [PubMed: 27095816]
4. Rosenblatt KP, Sun Z-P, Heller S, and Hudspeth AJ (1997). Distribution of Ca²⁺-Activated K⁺ Channel Isoforms along the Tonotopic Gradient of the Chicken's Cochlea. *Neuron* 19, 1061–1075. [PubMed: 9390519]
5. Davis RL (2003). Gradients of neurotrophins, ion channels, and tuning in the cochlea. *The Neuroscientist : a review journal bringing neurobiology, neurology and psychiatry* 9, 311–316.
6. Ricci AJ, Crawford AC, and Fettkoppe R (2003). Tonotopic variation in the conductance of the hair cell mechanotransducer channel. *Neuron* 40, 983–990. [PubMed: 14659096]
7. Nakamura W, Yamazaki S, Takasu NN, Mishima K, and Block GD (2005). Differential response of Period 1 expression within the suprachiasmatic nucleus. *The Journal of neuroscience : the official journal of the Society for Neuroscience* 25, 5481–5487. [PubMed: 15944376]

8. Yamaguchi S, Isejima H, Matsuo T, Okura R, Yagita K, Kobayashi M, and Okamura H (2003). Synchronization of Cellular Clocks in the Suprachiasmatic Nucleus. *Science* 302, 1408–1412. [PubMed: 14631044]
9. Haggerty HS, Lusted HS, and Morton SC (1993). Statistical quantification of 24-hour and monthly variabilities of spontaneous otoacoustic emission frequency in humans. *Hearing research* 70, 31–49. [PubMed: 8276731]
10. Yoo SH, Yamazaki S, Lowrey PL, Shimomura K, Ko CH, Buhr ED, Siepkas SM, Hong HK, Oh WJ, Yoo OJ, et al. (2004). PERIOD2::LUCIFERASE real-time reporting of circadian dynamics reveals persistent circadian oscillations in mouse peripheral tissues. *Proceedings of the National Academy of Sciences of the United States of America* 101, 5339–5346. [PubMed: 14963227]
11. Abraham U, Prior JL, Granados-Fuentes D, Piwnicka-Worms DR, and Herzog ED (2005). Independent circadian oscillations of Period1 in specific brain areas in vivo and in vitro. *The Journal of neuroscience : the official journal of the Society for Neuroscience* 25, 8620–8626. [PubMed: 16177029]
12. Welsh DK, Yoo S-H, Liu AC, Takahashi JS, and Kay SA (2004). Bioluminescence Imaging of Individual Fibroblasts Reveals Persistent, Independently Phased Circadian Rhythms of Clock Gene Expression. *Current Biology* 14, 2289–2295. [PubMed: 15620658]
13. Lande-Diner L, Stewart-Ornstein J, Weitz CJ, and Lahav G (2015). Single-cell analysis of circadian dynamics in tissue explants. *Molecular biology of the cell* 26, 3940–3945. [PubMed: 26269583]
14. Guilding C, Hughes AT, Brown TM, Namvar S, and Piggins HD (2009). A riot of rhythms: neuronal and glial circadian oscillators in the mediobasal hypothalamus. *Molecular Brain* 2, 1–19. [PubMed: 19138433]
15. Guilding C, Hughes ATL, and Piggins HD (2010). Circadian oscillators in the epithalamus. *Neuroscience* 169, 1630–1639. [PubMed: 20547209]
16. Landgraf D, Long JE, and Welsh DK (2016). Depression-like behaviour in mice is associated with disrupted circadian rhythms in nucleus accumbens and periaqueductal grey. *The European journal of neuroscience* 43, 1309–1320. [PubMed: 26414405]
17. Guilding C, and Piggins HD (2007). Challenging the omnipotence of the suprachiasmatic timekeeper: are circadian oscillators present throughout the mammalian brain? *The European journal of neuroscience* 25, 3195–3216. [PubMed: 17552989]
18. Evans JA (2016). Collective timekeeping among cells of the master circadian clock. *J Endocrinol* 230, R27–49. [PubMed: 27154335]
19. Lundkvist GB, Kwak Y, Davis EK, Tei H, and Block GD (2005). A calcium flux is required for circadian rhythm generation in mammalian pacemaker neurons. *The Journal of neuroscience : the official journal of the Society for Neuroscience* 25, 7682–7686. [PubMed: 16107654]
20. Mohawk JA, Green CB, and Takahashi JS (2012). Central and peripheral circadian clocks in mammals. *Annu Rev Neurosci* 35, 445–462. [PubMed: 22483041]
21. Brancaccio M, Patton AP, Chesham JE, Maywood ES, and Hastings MH (2017). Astrocytes Control Circadian Timekeeping in the Suprachiasmatic Nucleus via Glutamatergic Signaling. *Neuron* 93, 1420–1435.e1425. [PubMed: 28285822]
22. Tso CF, Simon T, Greenlaw AC, Puri T, Mieda M, and Herzog ED (2017). Astrocytes Regulate Daily Rhythms in the Suprachiasmatic Nucleus and Behavior. *Curr Biol* 27, 1055–1061. [PubMed: 28343966]
23. Yamazaki S, and Takahashi JS (2005). Real-time luminescence reporting of circadian gene expression in mammals. *Methods Enzymol* 393.
24. Nagano M, Adachi A, Nakahama K, Nakamura T, Tamada M, Meyer-Bernstein E, Sehgal A, and Shigeyoshi Y (2003). An abrupt shift in the day/night cycle causes desynchrony in the mammalian circadian center. *The Journal of neuroscience : the official journal of the Society for Neuroscience* 23, 6141–6151. [PubMed: 12853433]
25. Albus H, Vansteensel MJ, Michel S, Block GD, and Meijer JH (2005). A GABAergic mechanism is necessary for coupling dissociable ventral and dorsal regional oscillators within the circadian clock. *Current biology : CB* 15, 886–893. [PubMed: 15916945]

26. Ruan GX, Allen GC, Yamazaki S, and McMahon DG (2008). An autonomous circadian clock in the inner mouse retina regulated by dopamine and GABA. *PLoS biology* 6, e249. [PubMed: 18959477]
27. Anselmi F, Hernandez VH, Crispino G, Seydel A, Ortolano S, Roper SD, Kessar N, Richardson W, Rickheit G, Filippov MA, et al. (2008). ATP release through connexin hemichannels and gap junction transfer of second messengers propagate Ca²⁺ signals across the inner ear. *Proceedings of the National Academy of Sciences of the United States of America* 105, 18770–18775. [PubMed: 19047635]
28. Johnson SL, Forge A, Knipper M, Munkner S, and Marcotti W (2008). Tonotopic variation in the calcium dependence of neurotransmitter release and vesicle pool replenishment at mammalian auditory ribbon synapses. *J Neurosci* 28, 7670–7678. [PubMed: 18650343]
29. Cho S, and von Gersdorff H (2014). Proton-mediated block of Ca²⁺ channels during multivesicular release regulates short-term plasticity at an auditory hair cell synapse. *J Neurosci* 34, 15877–15887. [PubMed: 25429130]
30. Corns LF, Johnson SL, Kros CJ, and Marcotti W (2014). Calcium entry into stereocilia drives adaptation of the mechano-electrical transducer current of mammalian cochlear hair cells. *Proc Natl Acad Sci U S A* 111, 14918–14923. [PubMed: 25228765]
31. Mammano F, and Bortolozzi M (2017). Ca²⁺ signaling, apoptosis and autophagy in the developing cochlea: Milestones to hearing acquisition. *Cell calcium*.
32. Allen CN, Nitabach MN, and Colwell CS (2017). Membrane Currents, Gene Expression, and Circadian Clocks. *Cold Spring Harbor perspectives in biology* 9.
33. Colwell CS (2011). Linking neural activity and molecular oscillations in the SCN. *Nature reviews. Neuroscience* 12, 553–569. [PubMed: 21886186]
34. Marcotti W, Johnson SL, and Kros CJ (2004). Effects of intracellular stores and extracellular Ca(2+) on Ca(2+)-activated K(+) currents in mature mouse inner hair cells. *The Journal of physiology* 557, 613–633. [PubMed: 15064328]
35. Dawkins R, and Sewell WF (2004). Afferent synaptic transmission in a hair cell organ: pharmacological and physiological analysis of the role of the extended refractory period. *Journal of neurophysiology* 92, 1105–1115. [PubMed: 15056680]
36. Blanchet C, and Dulon D (2001). Tetraethylammonium ions block the nicotinic cholinergic receptors of cochlear outer hair cells. *Brain Res* 915, 11–17. [PubMed: 11578615]
37. Kuhlman SJ, and McMahon DG (2004). Rhythmic regulation of membrane potential and potassium current persists in SCN neurons in the absence of environmental input. *The European journal of neuroscience* 20, 1113–1117. [PubMed: 15305881]
38. Nitabach MN, Blau J, and Holmes TC (2002). Electrical silencing of *Drosophila* pacemaker neurons stops the free-running circadian clock. *Cell* 109, 485–495. [PubMed: 12086605]
39. Reijntjes DO, and Pyott SJ (2016). The afferent signaling complex: Regulation of type I spiral ganglion neuron responses in the auditory periphery. *Hear Res* 336, 1–16. [PubMed: 27018296]
40. Jagger DJ, and Forge A (2015). Connexins and gap junctions in the inner ear--it's not just about K(+) recycling. *Cell and tissue research* 360, 633–644. [PubMed: 25381570]
41. Eilers PH (2003). A perfect smoother. *Analytical chemistry* 75, 3631–3636. [PubMed: 14570219]
42. Savelyev SA, Larsson KC, Johansson AS, and Lundkvist GB (2011). Slice preparation, organotypic tissue culturing and luciferase recording of clock gene activity in the suprachiasmatic nucleus. *Journal of visualized experiments : JoVE*.
43. Park JS, Cederroth CR, Basinou V, Meltser I, Lundkvist G, and Canlon B (2016). Identification of a Circadian Clock in the Inferior Colliculus and Its Dysregulation by Noise Exposure. *The Journal of neuroscience : the official journal of the Society for Neuroscience* 36, 5509–5519. [PubMed: 27194331]

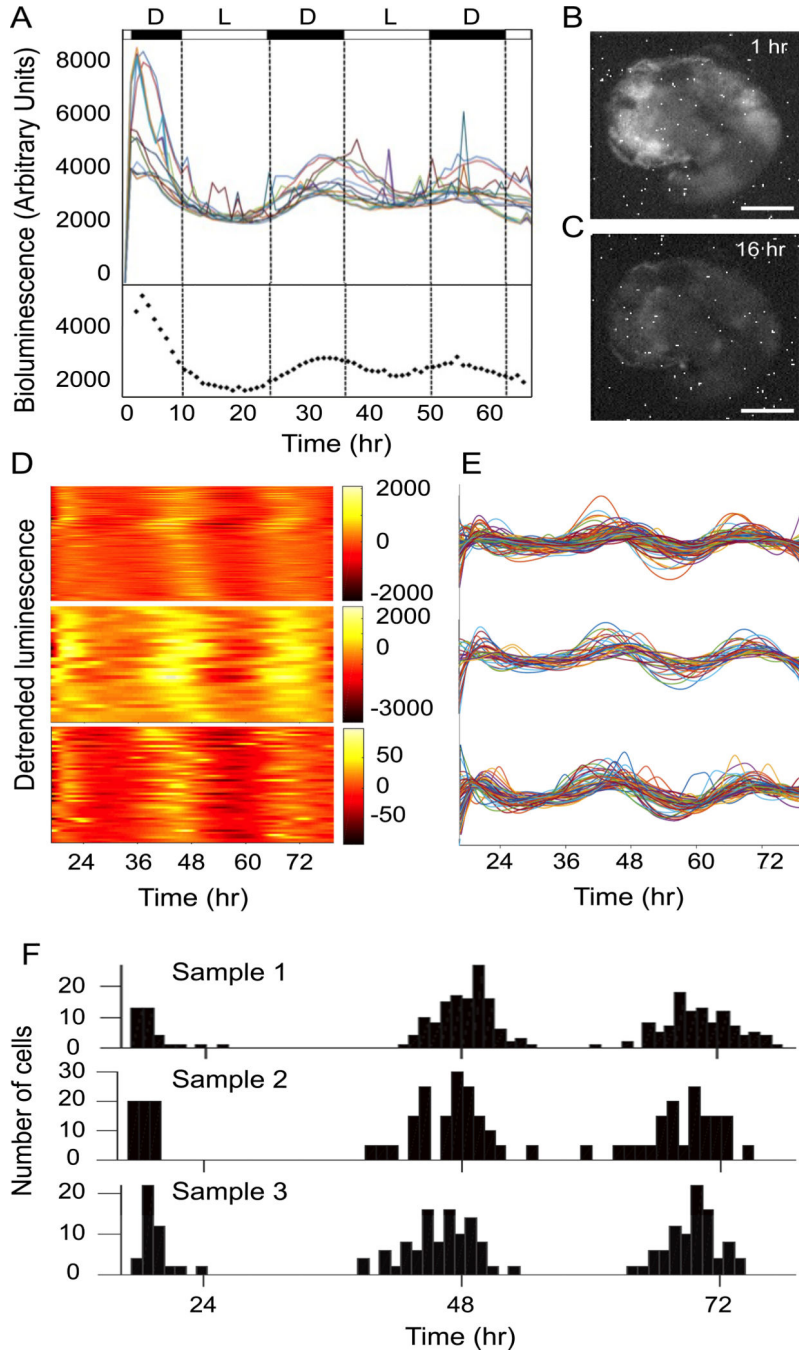


Figure 1. Robust cell-autonomous *PER2::LUC* rhythms in the cochlea.

(A) Top: Temporal changes of bioluminescence intensity in 13 different regions of interest (ROI) within a cochlear preparation. Bottom: The dotted line shows the average bioluminescence intensity. The black and white bars above the figure indicate the light (L) and dark (D) periods of the day respectively. (B) Bioluminescence image of the cochlea preparation after 1 h of recording (17:00 local time), corresponding to the peak *PER2* expression. (C) Bioluminescence image of the cochlea preparation after 16 h of recording (08:00 local time), corresponding to the trough *PER2* expression. (D-F) Bioluminescence

imaging and single unit analysis of circadian rhythms in 3 representative samples, revealed circadian patterns of PER2 expression. (D) Heat map showing peak (yellow) and trough (orange) luminescence intensity throughout the circadian cycle, over 72 hours of recordings. (E) Line plots of individual cell oscillators within the preparation. Each individual oscillator is depicted with a different color. (F) Distributions of peak expression time in the three circadian cycles that were recorded. Scale bar: 200 μm for (B) and (C). See also Figure S1 and movie S1.

Author Manuscript

Author Manuscript

Author Manuscript

Author Manuscript

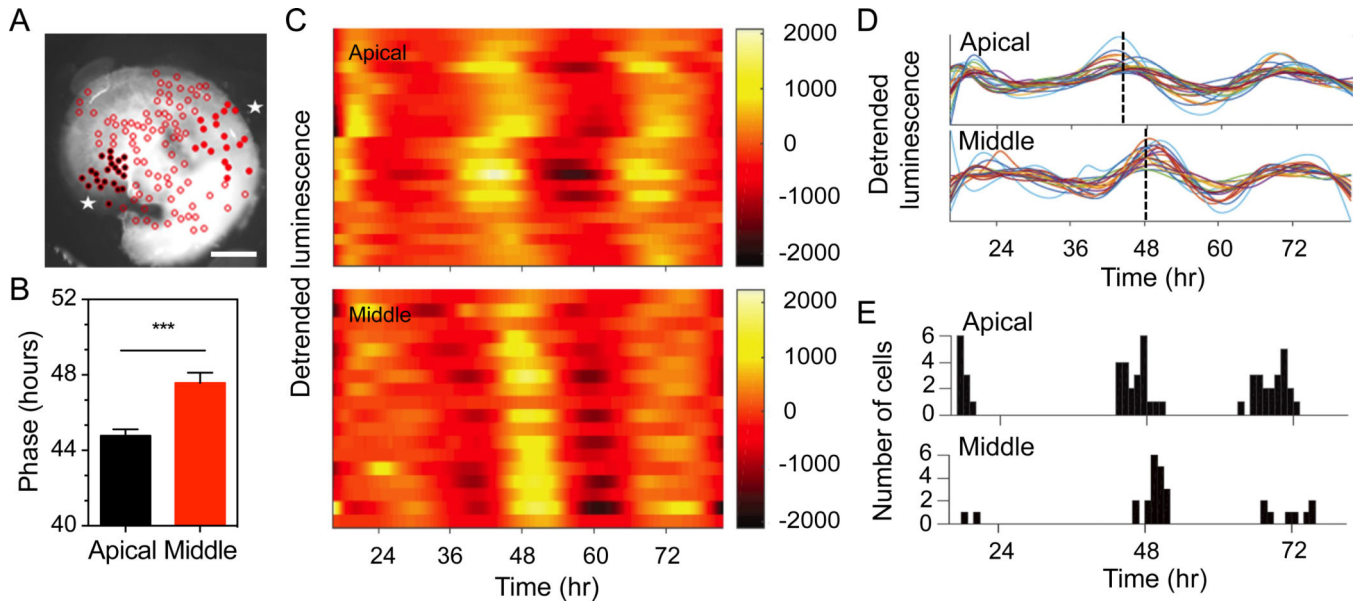


Figure 2. Tonotopical arrangement of circadian cell rhythms in the cochlea.

Temporal changes in bioluminescence monitored in individual cells located in the apical and middle cochlear regions. (A) Bioluminescence image of the cochlea preparation from the apical and middle regions as indicated by asterisks. The selection of cell populations is shown with black full circles for the apical turn and red full circles for the middle turn. Open circles indicate cells that were not analyzed. (B) Quantification of PER2::LUC phase in the apical and middle turn cell populations from 3 different preparations (mean \pm SEM, $n = 36-56$ cells, *** = $p < 0.001$ by t-test). (C) Representative heat maps of apical and middle cell populations, showing peak (yellow) and trough (orange) luminescence intensity throughout the circadian cycle, over 72 hours of recordings. (D) Line plots of individual cell oscillators in apical and middle turn. The dashed lines indicate average peak phase time in the apical and middle regions. (E) Distribution of peak time in each circadian cycle of recordings. Scale bar: 200 μm for (A).

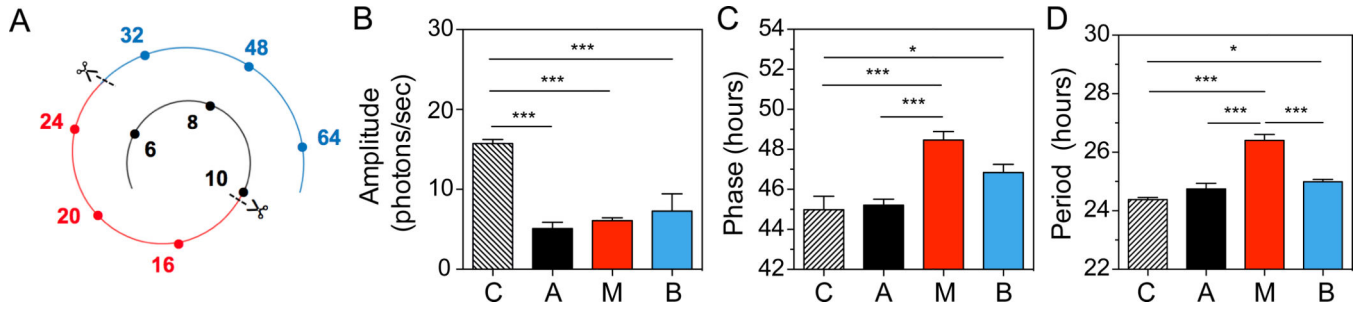


Figure 3. Contribution of the three cochlear regions in the generation of cochlear *PER2* rhythms. (A) Frequency regions selected for *PER2::LUC* monitoring are depicted (black: apical turn; red: middle turn; blue: basal turn). Scissors indicate the areas where the cochlea was cut and the numbers represent the corresponding frequencies along the tonotopic axis (kHz). (B) Amplitude, (C) phase and (D) period of *PER2::LUC* rhythms in the three different cochlear regions as depicted in the diagram (C: whole cochlea, A: apical turn, M: middle turn and B: basal turn). The color of each histogram corresponds to the frequency region shown in Fig. 3A. The results are presented as mean \pm SEM, $n = 7-13$ cochleae, * = $p < 0.05$, *** = $p < 0.001$.

Author Manuscript

Author Manuscript

Author Manuscript

Author Manuscript

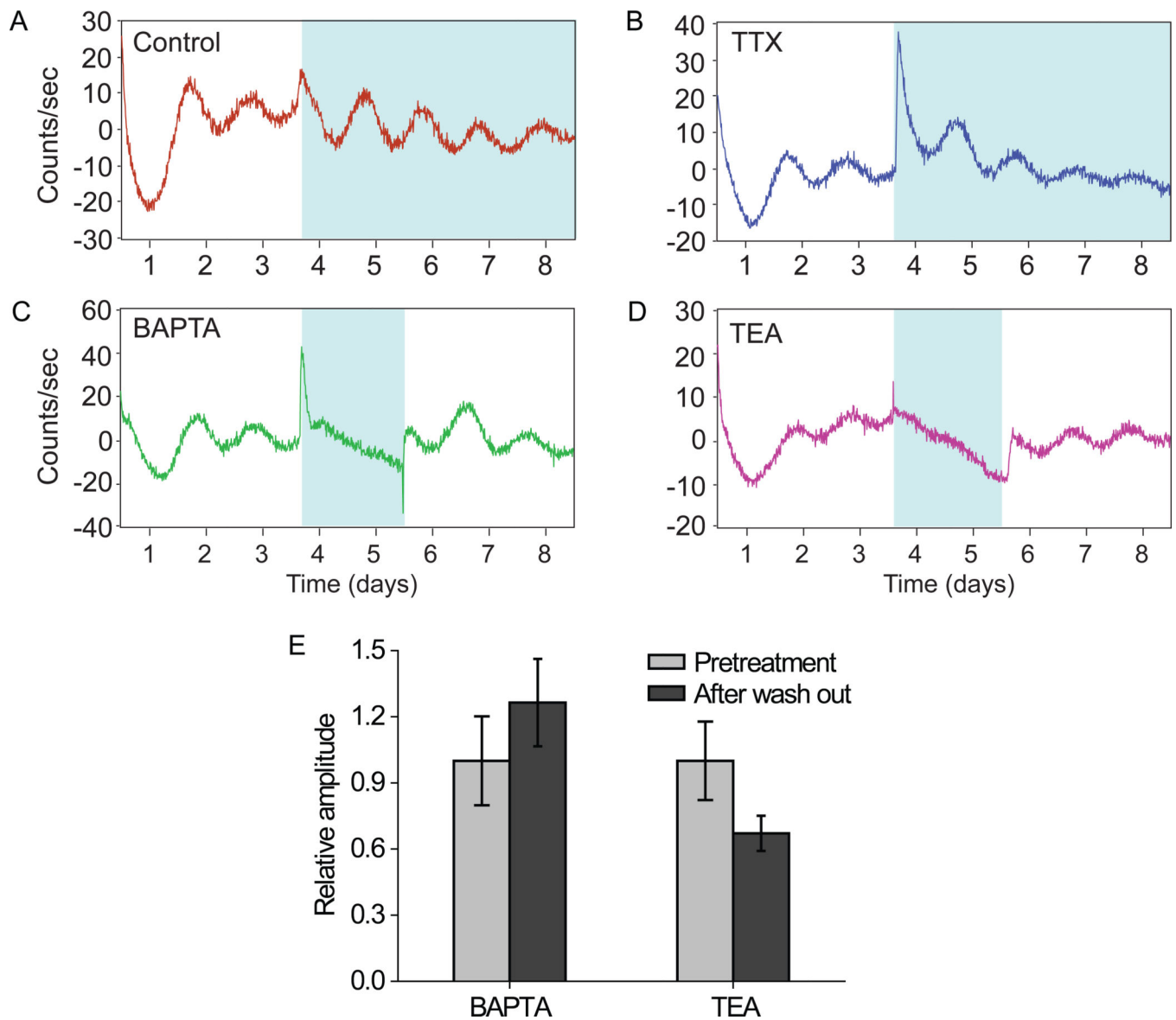


Figure 4. Contribution of various types of ion channels in the generation of cochlear PER2 rhythms.

(A-D) Disappearance of cochlear PER2::LUC rhythms after BAPTA or TEA treatment with re-establishment of the oscillatory activity after washout. Cochlear explants were treated with BAPTA (4 mM; C) or TEA (25 mM; D) for a period of 2 days (blue shading) and then the culture medium was replaced by fresh medium. For cochlear explants treated with vehicle (A) or TTX (40 μ M; B), the culture medium was not replaced by fresh medium for a period of 5 days (blue shading). (E) Comparison of amplitudes of pre- and post-treatment. The results are presented as mean \pm SEM, $n = 4-11$ cochleae. See also Figure S2.